ISSN 1674-1056
http://cpb.iphy.ac.cn
http://iopscience.iop.org/cpb
中国物理 B
Chinese Physics
中国物理 Chinese Physics B

Hot spots enriched plasmonic nanostructure-induced random lasing of quantum dots thin film

Feng Shan(单锋), Xiao-Yang Zhang(张晓阳), Jing-Yuan Wu(吴静远), Tong Zhang(张彤)
Citation: Chin. Phys. B . 2018, 27(4): 047804. **doi:** 10.1088/1674-1056/27/4/047804

Journal homepage: http://cpb.iphy.ac.cn; http://iopscience.iop.org/cpb

What follows is a list of articles you may be interested in

Optical response of tunable terahertz plasmon in a grating-gated graphene transistor

Bo Yan(闫博), Jingyue Fang(方靖岳), Shiqiao Qin(秦石乔), Yongtao Liu(刘永涛), Li Chen(陈力), Shuang Chen(陈爽), Renbing Li(李仁兵), Zhen Han(韩震)
Chin. Phys. B . 2017, 26(9): 097802. **doi:** 10.1088/1674-1056/26/9/097802

Super scattering phenomenon in active spherical nanoparticles

Chang-Yu Liu(刘昌宇), Ya-Ming Xie(解亚明), Zhi-Guo Wang(王治国)
Chin. Phys. B . 2017, 26(6): 067803. **doi:** 10.1088/1674-1056/26/6/067803

Effects of thickness & shape on localized surface plasmon resonance of sexfoil nanoparticles

Yan Chen(陈艳), Xianchao Liu(刘贤超), Weidong Chen(陈卫东), Zhengwei Xie(谢征微), Yuerong Huang(黄跃容), Ling Li(李玲)
Chin. Phys. B . 2017, 26(1): 017807. **doi:** 10.1088/1674-1056/26/1/017807

Restructuring of plasmonic nanoparticle aggregates with arbitrary particle size distribution in pulsed laser fields

A E Ershov, A P Gavrilyuk, S V Karpov, S P Polyutov
Chin. Phys. B . 2016, 25(11): 117806. **doi:** 10.1088/1674-1056/25/11/117806

Exchange effect and magneto-plasmon mode dispersion in an anisotropic two-dimensional electronic system

Xiaoguang Wu(吴晓光)
Chin. Phys. B . 2016, 25(11): 117801. **doi:** 10.1088/1674-1056/25/11/117801

Hot spots enriched plasmonic nanostructure-induced random lasing of quantum dots thin film*

Feng Shan(单锋)[1,3], Xiao-Yang Zhang(张晓阳)[1,2,3], Jing-Yuan Wu(吴静远)[1,3], and Tong Zhang(张彤)[1,2,3,†]

[1] *Joint International Research Laboratory of Information Display and Visualization, School of Electronic Science and Engineering, Southeast University, Nanjing* 210096, *China*

[2] *Key Laboratory of Micro-Inertial Instrument and Advanced Navigation Technology, Ministry of Education, and School of Instrument Science and Engineering, Southeast University, Nanjing* 210096, *China*

[3] *Suzhou Key Laboratory of Metal Nano-Optoelectronic Technology, Suzhou Research Institute of Southeast University, Suzhou* 215123, *China*

(Received 23 December 2017; revised manuscript received 31 January 2018; published online 10 March 2018)

Here, a plasmon-enhanced random laser was achieved by incorporating gold nanostars (NS) into disordered polymer and CdSe/ZnS quantum dots (QDs) gain medium films, in which the surface plasmon resonance of gold NS can greatly enhance the scattering cross section and bring a large gain volume. The random distribution of gold NS in the gain medium film formed a laser-mode resonator. Under a single-pulse pumping, the scattering center of gold NS-based random laser exhibits enhanced performance of a lasing threshold of 0.8 mJ/cm^2 and a full width as narrow as 6 nm at half maximum. By utilizing the local enhancement characteristic of the electric field at the sharp apexes of the gold NS, the emission intensity of the random laser was increased. In addition, the gold NS showed higher thermal stability than the silver nanoparticles, withstanding high temperature heating up to 200 °C. The results of metal nanostructures with enriched hot spots and excellent temperature stability have tremendous potential applications in the fields of biological identification, medical diagnostics, lighting, and display devices.

Keywords: plasmon, gain medium, gold nanostars, random laser

PACS: 78.67.Bf, 78.68.+m, 73.21.La, 42.55.Zz **DOI:** 10.1088/1674-1056/27/4/047804

1. Introduction

Compared with the conventional lasers requiring precise fabrication and strict alignment of reflective resonator cavities, the random lasers can be realized by randomly formed closed-loop cavities with metal nanoparticles (MNP) or high refractive index dielectric nanoparticles (DNP) embedded in the gain media.[1–4] The random lasers mainly utilize the interaction between the light and the disordered gain media, thus emitting the light with high intensity and narrow spectral line. Because of the simple fabrication process and low cost, they have potential applications in many fields, including temperature sensors, lighting and display devices, biological identification and medical diagnostics.[5–8] To obtain random lasing, the scattering intensity of the gain medium should be as large as possible to achieve a larger gain volume.[9] In previous random laser studies, researchers usually use DNP with high refractive index and good scattering ability as scatterers, such as TiO_2, SiO_2, ZnO, and so on.[10–13] The scattering intensity of this random laser can be enhanced by decreasing the average free path of scattering, thus reducing the threshold of random laser and obtaining the random laser with higher intensity. In order to reduce the average free path of scattering, it is necessary to increase the scattering cross-section or the concentration of DNP.[10,12] However, the larger size or higher concentration of DNP will easily lead to aggregation and precipitation, and the stability of the system cannot be guaranteed.[12] Worse still, some DNP have a significant photo-degradation effect on the gain medium, for example, when TiO_2 was used as scatters, the intensity of the output random laser is only one-fifth of the initial value after 4500 pump pulses.[10]

Recently, MNPs have attracted a great deal of attention for their unique localized surface plasmon resonance (LSPR) properties.[14–18] Compared with DNP, MNP have significant advantages. The scattering cross-section of MNP in visible light is much larger than that of DNP with the same size, especially when the particle size is less than 100 nm. Researchers usually choose silver nanoparticles when using MNP to enhance fluorescence emission because silver has better LSPR properties in visible light.[19–21] However, the thermal stability of silver is a great challenge in the laser excitation experiment, because the pump source generates great heat by high pulse energy. At present, the thermal stability of silver nanoparticles has been studied both theoretically and experimentally.[22–24] The results showed that the morphology of silver nanopar-

*Project supported by the National Key Research and Development Program of China (Grant No. 2017YFA0205800), the National Natural Science Foundation of China (Grant Nos. 11734005, 61307066, and 61450110442), the Natural Science Foundation of Jiangsu Province, China (Grant No. BK20130630), the Doctoral Fund of Ministry of Education of China (Grant No. 20130092120024), the Innovation Fund of School of Electronic Science and Engineering, Southeast University, China (Grant No. 2242015KD006), and the Scientific Research Foundation of Graduate School of Southeast University, China (Grant Nos. YBJJ1513 and YBJJ1613).

†Corresponding author. E-mail: tzhang@seu.edu.cn

© 2018 Chinese Physical Society and IOP Publishing Ltd

ticles became deformed at 95 °C for 10 min.[24] Therefore, the silver nanoparticles cannot meet the need of some lasing experiments with ultra-high pump pulse energy. However, gold nanostructures showed extremely high thermal stability, which was an ideal choice for laser experiment. In Xia's experiment,[25] the fragmentation of the gold plates was not seen until heating at a temperature of more than 450 °C. However, the thermal stability of nanostructure with enrich hot spots is rarely studied. Hot spots can produce a strong local electric field,[26,27] which greatly enhances the emission characteristics of the gain medium, especially for random laser.[17] The hot spot effect of MNP is closely related to their morphology, size, and composition.[28–31] At present, researchers have exerted a great deal of effort in the preparation of high-yield metal nanostructures with controllable morphology, which is also a field worthy of research.[32] Therefore, advanced engineering to obtain metal nanostructures with enriched hot spots and to further study MNP's thermal stability are of current interest for exploration.

In this paper, we demonstrated a type of random laser in the gain medium film by introducing an enriched nanostructure as scatterer. The synthesized gold nanostars (NS) nanostructure with the apexes structure have a hot spot effect due to the strong electric field distributed at its sharp apexes, which lead to plasmon scattering enhancement. The heating experiments of the gold NS show that the apexes structure of the gold NS still keeps stable at 200 °C. The realization of random lasing is mainly attributed to the remarkable scattering of gold NS in the system. For our random laser system, in which gold NS are used as scatters, a random lasing with a bandwidth of 6 nm is obtained. The results reported here provide a straightforward and simple method for plasmon random lasers with multiple scattering based on complex morphologic scatterers.

2. Experimental details

2.1. Materials

Polyvinyl pyrrolidone (PVP, MW ∼29000), silver nitrate ($AgNO_3$, $>$ 99.9%) and ascorbic acid (AA, $>$ 99.5%) were purchased from Sigma–Aldrich, USA. Gold chloride trihydrate ($HAuCl_4{\cdot}3H_2O$, $>$ 99.9%) and hydrochloric acid (HCl, $>$ 98.0%) were purchased from Sinopharm Chemical Reagent Co., Ltd., China. The CdSe/ZnS quantum dots (QDs) solution was purchased from the Suzhou Xingshuo Nanotech Co., Ltd., China. Ultrapure water from Milli-Q (Millipore, USA, resistivity $>$ 18.4 MΩ· cm) source was used throughout the experiments.

2.2. Characterization

The structural features of the gold seeds, NS and CdSe/ZnS QDs were detected with scanning electron microscope (SEM, Zeiss Ultra Plus, Germany) and transmission electronic microscopy (TEM; Fei Tecnai T20, USA). Extinction spectra were measured with the fiber optic spectrometer (NOVA, Ideaoptics Technology Ltd., China). The femtosecond Ti:Sapphire laser system (Legend-F-1k, 800 nm, 1 kHz, 100 fs) was used in the excitation pulses experiment. The 400-nm pumping beam was realized through a β-barium borate (BBO) crystal. A fast optical multichannel analyzer (OMA, Spectra Pro-300i) was used to collect the emitted beam at the edge of the sample.

2.3. Fabrication of gold seeds

A 100-mL solution with concentration of 1-mmol/L $HAuCl_4{\cdot}3H_2O$ solution was heated to boiling. Then 15-mL trisodium citrate solution with a mass fraction of 1% under vigorous stirring was added. The gold seed solution was obtained by heating the reaction solution for 15 minutes, then reserved after cooling.

2.4. Fabrication of gold NS and gold NS film

A 100-μL HCl solution with 1-mol/L concentration and 1-mL seeds solution were added to 100-mL $HAuCl_4{\cdot}3H_2O$ solution with 0.25-mmol/L concentration in turn under stirring of 700 rpm. Then, 1-mL $AgNO_3$ solution with 30-mmol/L concentration and 500-μL AA solution with 100-mmol/L concentration were added simultaneously. After 30-s reaction, the color of the solution changed rapidly, and finally the gold NS samples were obtained. Finally, the gold NS solution was centrifuged at 4500 rpm for 45 minutes, then the precipitate was re-dispersed into 10-mL water.

A rapid assistance-free self-assembly method was used for the fabrication of gold NS film. A pre-cleaned indium tin oxide (ITO) glass slab was put into the untreated gold NS solution. After 12 h, the ITO glass slab was removed from the solution and the surface was flushed with water. Finally, the gold NS thin film was fabricated for the thermal stability experiment.

2.5. Fabrication of gain medium thin film

The 0.7-mL CdSe/ZnS QDs ethanol solution with 0.3 mg/mL was fully mixed with 0.1-g PVP and stirred for 30 min at 600 rpm. Then 300-μL ultrasonic treated gold NS solution was added to the mixed solution. To prevent gold NS aggregation, the mixed solution was stirred for 1 h and then was left still for 12 h. Then the mixed solution was spinned onto the pre-cleaned ITO glass for 60 s at 3000 rpm. Finally, the prepared thin film sample was put into the drying box for 6 h at 60 °C. The PVP constituted a matrix for the CdSe/ZnS QDs gain medium and immobilized the embedded NPs in the dried thin film. The gold NSs were embedded and immobilized in a gain medium film composed of PVP and CdSe/ZnS QDs. Meanwhile, the film without gold NS was prepared under the same process conditions.

3. Results and discussion

3.1. Characterization of CdSe/ZnS QDs and gold seeds

The dispersion characteristics of QDs are very important for the preparation of uniform random laser gain medium thin films. To evaluate the dispersion of CdSe/ZnS QDs, we measured their dispersion properties using TEM, as shown in Fig. 1(a). The size of the CdSe/ZnS QDs displayed in the TEM image is remarkably uniform. The corresponding absorption (black line) and emission spectra (red line) of the CdSe/ZnS QDs are illustrated in Fig. 1(b). The emission peak of CdSe/ZnS QDs is located at $\sim$ 628 nm. The position of emission peak can be tuned by varying the size of CdSe/ZnS QDs.[33] To evaluate the gold seeds we synthesized, the morphologies of the gold seeds were measured by TEM, as shown in Fig. 1(c). The TEM image indicates the gold seeds that were monodispersed in the solution. To determine the size uniformity of the gold seeds, we made a statistical analysis of the particles size for the TEM image, as displayed in the inset of Fig. 1(c). The results indicated that the seed size is mainly between 20 nm and 30 nm. Then, by testing the absorption spectra of the gold seeds (Fig. 1(d)), we further studied their LSPR properties. As shown in Fig. 1(d), the LSPR peak of gold seeds is located at about 520 nm, which is consistent with the small nanospheres that we have observed.[34]

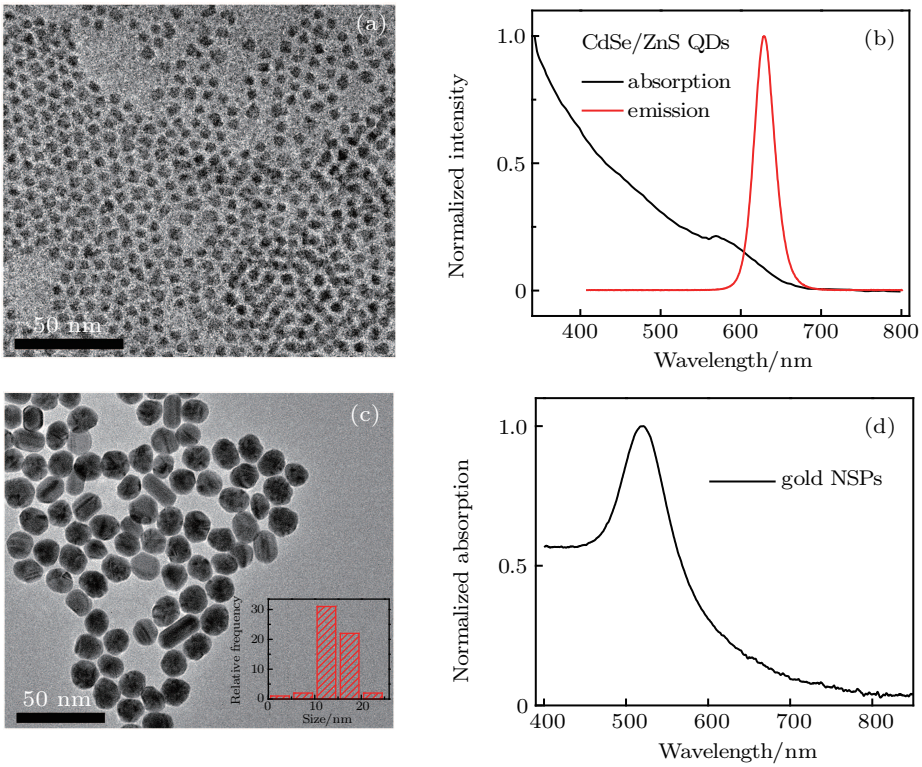


Fig. 1. (color online) (a) TEM image and (b) normalized absorption and emission spectra of the CdSe/ZnS QDs, and (c) TEM image and (d) normalized absorption spectrum of the gold seeds.

3.2. Characterization of gold NS

To obtain high-quality random laser, we prepared gold NS nanostructures with many sharp apexes by the seed-growth method. Figure 2(a) shows the TEM image of gold NS. As shown in Fig. 2(a), the gold NS was well dispersed and each particles had several apexes nanostructures distributed on the surface. To observe its microscopic morphology more clearly, the high magnification of single gold NS TEM image is shown in the inset of Fig. 2(a). The central nucleus's size of the gold NS is about 50 nm, while the sharp apexes are of varying lengths. This multi-tip nanostructure has a great scattering characteristic. The apexes position will produce a large number of hot spots. All of them can enhance the light emission of fluorophore. To estimate the LSPR properties of this kind of gold NS, we have further measured the absorption spectrum of the gold NS solution. As shown in Fig. 2(b), the LSPR peak of the gold NS is about 810 nm. Compared with the gold seeds, the LSPR peak of the gold NS has a remarkable red shift, which is due to the increase of particle size.

In our experiment, we used a typical vertical pumping, lateral detection experimental setup, as shown in Fig. 2(c). In the setup, the femtosecond Ti:sapphire laser system (Legend-F-1k, 800 nm, 1 kHz, 100 fs, Coherent, USA) was used as the pump light source. The 400-nm pumping beam was realized through a BBO crystal. In the signal detection, we use a fast optical multichannel analyzer (OMA, Spectra Pro-300i, Princeton instruments, USA) to collect the emitted beam at the edge of the sample. Meanwhile, a 532-nm high pass filter is used to suppress the scattering light from the pump light source.

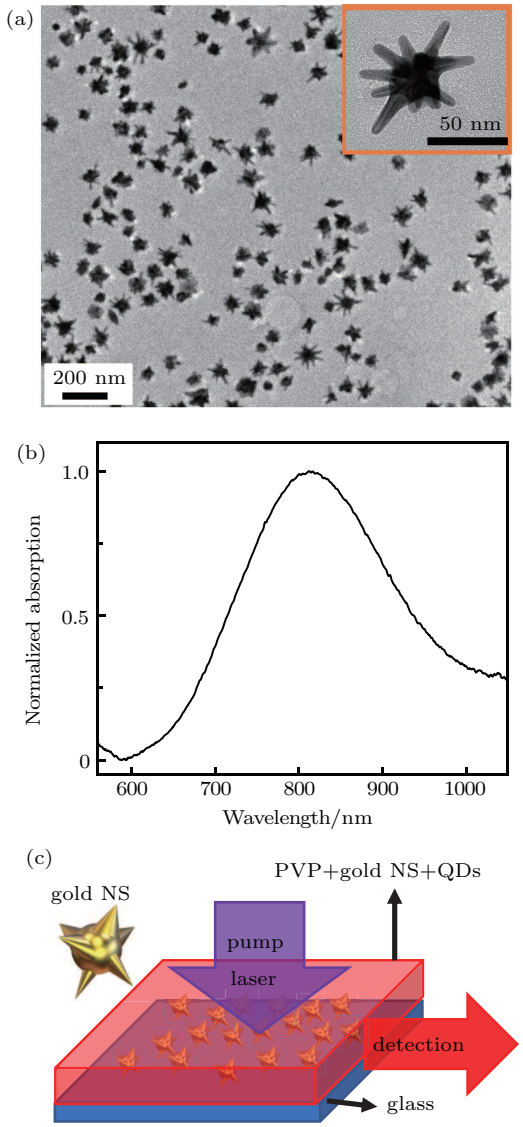


Fig. 2. (color online) (a) TEM image of the gold NS. The inset of panel (a) corresponds to higher magnification TEM image. (b) The normalized absorption spectra of gold nanostars (NS). (c) Illustration of the pump and detection of emission from the edge of the gain medium film.

3.3. Thermal stability of gold NS

Anisotropic MNP, especially those with lots of sharp-apex nanostructures, have strong near field enhancement properties due to their lightning rod effects.[35] However, the near field enhancement is also accompanied by the generation of heat, which will have an impact on metal nanostructures, especially on the sharp apexes.[36] Once the morphology of metal nanostructures degenerates due to the surrounding high-temperature environment, it will directly affect the stability of the system and even cause serious performance degradation. Therefore, it is necessary to check the relationship between the morphology of MNP and temperature, which can be used to guide some experiments related to high heat. We compared the SEM images of the gold NS at different annealing temperatures. It can be seen from Fig. 3(a) that when the gold NS was annealed at 150 °C, the morphology of the gold NS can still be maintained well compared with the TEM image in Fig. 2(a). With the increase of annealing temperature, the apexes morphology of the gold NS surface gradually degenerates. When annealed at a temperature of 250 °C, the apexes morphology of the gold NS surface has become less apparent, as shown in Fig. 3(c). Moreover, when the annealing temperature increased to 300 °C, the apexes nanostructures of the gold NS disappeared completely and transformed into nanospheres (Fig. 3(d)). The results indicate that the apexes nanostructures of the synthesized gold NS can keep its shape when annealing at 200 °C. Because Ag has a lower melting point than gold, Ag nanoparticles are more susceptible to temperature. The results in the literature showed that the morphology of Ag nanoparticles began to change when heating at 90 °C,[24] while that of gold NS changed at about 200 °C. Therefore, we believe that the gold material is more suitable than silver for some experiments in high temperature environment.

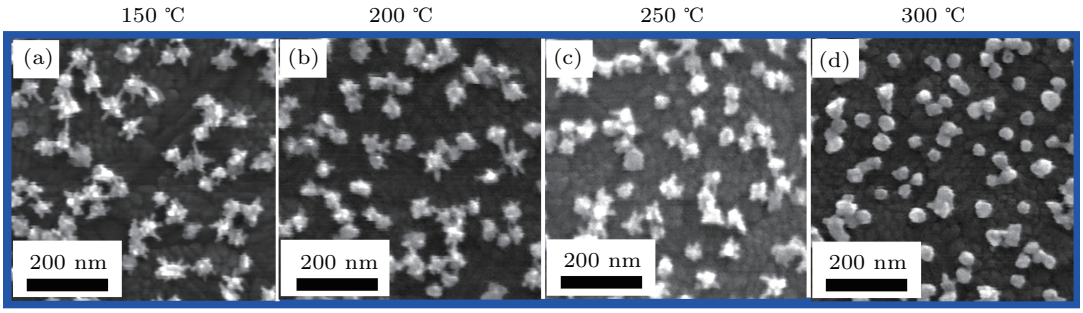


Fig. 3. (color online) SEM images of the gold NS films after annealing in air atmospheres. The samples were annealed at: (a) 150 °C, (b) 200 °C, (c) 250 °C, and (d) 300 °C for 5 minutes, respectively.

3.4. Characterization of random laser

To demonstrate the emission properties of the CdSe/ZnS QDs doped random laser sample with gold NS as scatters, we have carried out experimental measurement on them. The random lasing spectrum collected at different pump fluences is shown in Fig. 4(a). In Fig. 4(a), we only observe the emission of the fluorescence signal at low pump fluences (below the threshold). When the pump fluences are higher than the laser threshold (0.8 mJ/cm^2), the single-mode random lasing signals were detected. The random lasing comes from the incoherent feedback in the device. With the increase of pump fluences, the random lasing was obtained when the gain

is greater than the loss. Meanwhile, the full width at half maximum (FWHM) of random lasing becomes narrower with the increase of pump fluences. The apex nanostructure of a gold nanostar (NS) has a large number of hot spots; many investigations[37,38] have proved that the electromagnetic enhancement factor of spots can reach more than 10^9. Therefore, the hot spot effect produced by the gold NS can greatly enhance the emission efficiency of QDs, thus enhancing the random laser signal. In our study, the surface plasmon resonance spectrum of the gold NS is not overlapping completely well with the emission wavelength band of QDs. The reason is due to the complex morphology and anisotropic apex distribution. As a result, the resonant wavelengths of different hot spots on the gold NS are completely different. This will lead to the resonance peaks spreading in a wide wavelength range corresponding to different dipole moments. Although their resonance wavelengths depend on the macroscopical distribution of average size, which is not overlapping completely with the emission wavelength of QDs, it still enables the generation of many hot spots contributing to the electromagnetic enhancement at the emission wavelength.

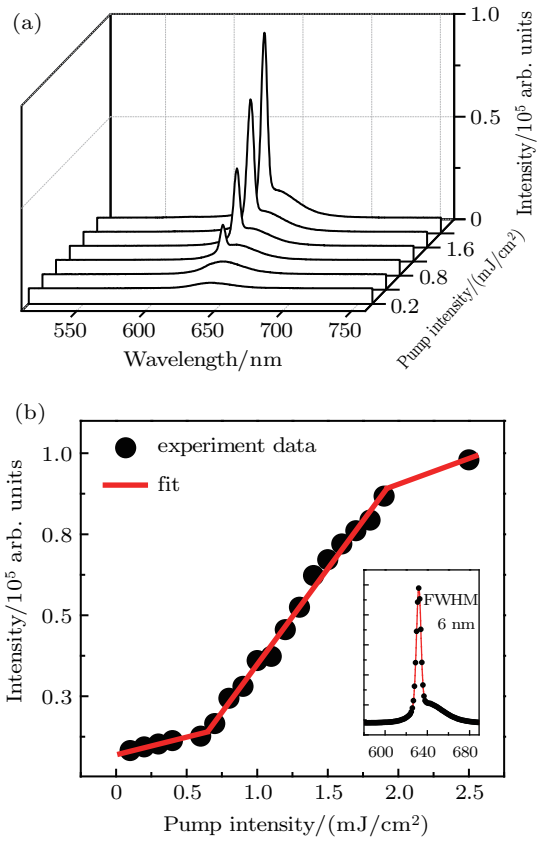


Fig. 4. (color online) (a) Lasing emission spectra of the gain medium film with gold NS under different pump fluences. (b) Lasing emission intensity as a function of the increasing pump fluence. The inset shows that the FWHM of lasing emission peak is 6 nm.

To evaluate the effect of pump fluence on the intensity of emission, we further studied the relationship between them, as shown in Fig. 4(b). As can be seen from Fig. 4(b), when the pump fluence exceeds the threshold value 0.8 mJ/cm^2, the emission intensity shows a steep linear increase. However, with the increase of the pump fluence, the emission intensity reaches a saturation state, and the increasing trend becomes slower. We believe that the reasons for this saturation phenomenon are as follows. During the process of random laser pumping, both Auger recombination and optical gain amplification exist. When the pump fluence is low, the Auger recombination effect is very small, and the optical gain amplification is dominant for the device. However, with the increase of pump fluence, more electrons will reverse to high energy levels. When the number of electrons in the high energy level reaches a certain number, there will be a significant Auger recombination effect, and the recombination rate will increase rapidly with the increase of the number of electrons. When the pump fluence further increases, the Auger recombination and optical gain amplification effect will reach a dynamic equilibrium, and the random laser intensity will be saturated with the increase of the pump fluence.[39,40] As illustrated in the inset of Fig. 4(b), an FWHM of only 6 nm was obtained. We have calculated that the quality factor (Q) of the random is 105, according to $Q = \lambda/\Delta\lambda$, where λ and $\Delta\lambda$ are the wavelength and line width of the random lasing peak, respectively. The results indicate that the closed loop has a high Q.

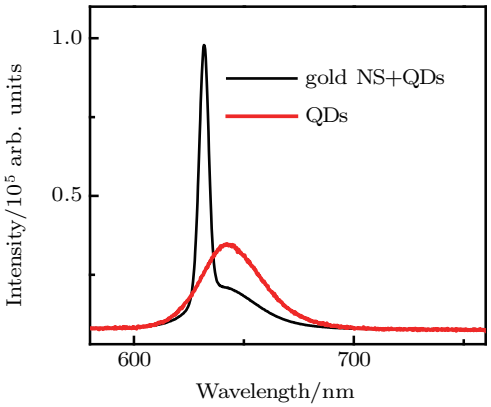


Fig. 5. (color online) Emission characteristics of gain medium thin films. For two films, spectra were recorded at the same pump fluence of 2.5 mJ/cm^2. The reference film without gold NS shows ASE (red line). The film containing gold NS exhibits high intensity lasing (black line).

To determine the role of gold NS in random laser devices, we have further studied a kind of reference sample, that is, disordered gain medium thin film without gold NS. The emission spectrum of the two samples at 2.5-mJ/cm^2 pumping fluence is displayed in Fig. 5. From Fig. 5, we can see clearly that for the sample without doping gold NS, the emission signal is the only fluorescence spectra. But when the gold NS were doped, we obtained a single-mode random lasing signal. Therefore, the gold NS act not only as scatterers, but also further enhance the emission of CdSe/ZnS QDs because of the strong electric field on the surface. In addition, during the process of synthesizing QDs, a layer of CdS was added before the shell fabrication for

ensuring the lattice matching between the CdSe core and the ZnS shell. In fact, in the random laser experiment, we adopted a quasi-type-II CdSe/ZnS core–shell QDs structure. For this quasi-type-II structure, there are spatially separated electrons and holes between the core and the shell structures. Because of the high local charge densities, the excitons are repulsive to each other, moving upward the Coulomb interaction energy of the exciton–exciton. Therefore, the emission of random laser is blue-shifted when it is pumped.[41,42]

4. Conclusion

In conclusion, we have fabricated high-yield gold NS nanostructures with lots of hot spots and high thermal stability. Then, we have successfully prepared single-mode random lasing with narrow line width using these excellent nanostructures. The plasma-enhanced scattering characteristics of gold NS provide an ideal result with a large scattering cross section, while the surface of gold NS will also produce a strong electric field enhancement because of the hot spot effect induced by the sharp apexes nanostructures. This will greatly enhance the emission characteristics of CdSe/ZnS QDs. Through thermal annealing experiments, we found that the thermal stability of the gold NS is extremely high and can withstand nearly a high temperature at 200 °C. The random laser threshold of 0.8 mJ/cm^2 is obtained by measuring the continuous pumping fluences of the sample. With increasing pump fluence, we have realized a random lasing with an FWHM of 6 nm. The comparative experiments show that the gold NS in this disordered gain medium is critical for the realization of random lasing. We expect these results will reward attempts to use plasmon-enhanced random lasing in temperature sensors, lighting, and display devices applications.

References

[1] Jiang X and Soukoulis C M 2000 *Phys. Rev. Lett.* **85** 70
[2] Apalkov V M, Raikh M E and Shapiro B 2002 *Phys. Rev. Lett.* **89** 016802
[3] Vanneste C, Sebbah P and Cao H 2007 *Phys. Rev. Lett.* **98** 143902
[4] Oleg Z and Lev D 2010 *J. Opt.* **12** 024001
[5] Cao H, Xu J Y, Seelig E W and Chang R P 2000 *Appl. Phys. Lett.* **76** 2997
[6] Stefano G, Stefano C, Oleg Y and Diederik S W 2004 *Phys. Rev. Lett.* **93** 263901
[7] Diederik S W and Stefano C 2001 *Nature* **414** 708
[8] Wiersma D S 2008 *Nat. Phys.* **4** 359
[9] Diederik S W and Lagendijk A 1996 *Phys. Rev. E* **54** 4256
[10] Takashi O and Shiro A 2010 *Opt. Rev.* **17** 300
[11] Brito A M, André G, Anderson S L, Alcenisio J J and Cid B A 2010 *J. Appl. Phys.* **108** 033508
[12] Kitur J, Zhu G, Bahoura M and Noginov M A 2010 *J. Opt.* **12** 024009
[13] Que M L, Wang X D, Peng Y Y and Pan C F 2017 *Chin. Phys. B* **26** 067301
[14] Zhang X Y, Hu A, Zhang T, Lei W, Xue X J, Zhou Y H and Duley W W 2011 *ACS Nano* **5** 9082
[15] Cho C Y and Park S J 2016 *Opt. Express* **24** 7488
[16] Shan F, Zhang X Y, Fu X C, Zhang L J, Su D, Wang S J, Wu J Y and Zhang T 2017 *Sci. Rep.* **7** 6813
[17] Li L, Daisi H, Wei B, Meng F, Peng Z, Dingke Z and Shi C 2017 *J. Alloys Compd.* **693** 876
[18] Zhai T, Chen J, Chen L, Wang J, Wang L, Liu D H, Li S, Liu H and Zhang X P 2015 *Nanoscale* **7** 2235
[19] Wang Z, Meng X, Seung H C, Sebastian K, Young L K, Hui C, Vladimir M S and Alexandra B 2016 *Nano Lett.* **16** 2471
[20] Tianrui Z, Xu Z, Xiao W, Yi W, Fei L and Xin Z 2016 *Opt. Express* **24** 437
[21] Qing C, Xiao S, Xuan L, Jun T, Da L and Zhao W 2017 *Nanophotonics* **6** 1151
[22] Yosia N W, Jinwoo K, Won M C, Sung H P and Mun H K 2017 *Nanoscale* **9** 11705
[23] Mahesh K G, Robert W J and Timothy L K 2016 *Dalton Trans.* **45** 9827
[24] Kee E L, Amelia V H and Timothy L K 2014 *Phys. Chem. Chem. Phys.* **16** 12407
[25] Cai K, Xiao Z and Guang W 2006 *J. Phys. Chem. B* **110** 4651
[26] Zhang X Y, Zhang T, Hu A, Song Y J and Duley W W 2012 *Appl. Phys. Lett.* **101** 153118
[27] Zhong H H, Zhou J H, Gu C J, Wang M, Fang Y T, Xu T and Zhou 2017 *Chin. Phys. B* **26** 127301
[28] Zhang X Y, Zhou H L, Shan F, Xue X M, Su D, Liu Y R, Chen Y Z, Wu J Y and Zhang T 2017 *RSC Adv.* **7** 55680
[29] Fan G H, Qu S L, Guo Z Y, Wang Q and Li Z G 2012 *Chin. Phys. B* **21** 047804
[30] Yan C, Liu X, Wei C, Zheng X, Yue H and Ling L 2017 *Chin. Phys. B* **26** 017807
[31] Shi X, Wang Y, Wang Z, Sun Y, Liu D H, Zhang Y, Li Q and Shi J W 2013 *Appl. Phys. Lett.* **103** 023504
[32] Zhang T, Song Y J, Zhang X Y and Wu J Y 2014 *Sensors* **14** 5860
[33] Peng Z A and Peng X 2001 *J. Am. Chem. Soc.* **123** 183
[34] Zhu S Q, Zhang T, Guo X L, Wang Q L, Liu X and Zhang X Y 2012 *Nanoscale Res. Lett.* **7** 613
[35] Johannes Z, Christian W, Cynthia V, Calin H and Thomas A K 2016 *ACS Photonics* **3** 919
[36] Zhang X Y, Shan F, Zhou H L, Su D, Xue X M, Wu J Y, Chen Y Z, Zhao N and Zhang T 2018 *J. Mater. Chem. C*
[37] Lee H, Kim G H, Lee J H, Kim N H, Nam J M and Sun Y D 2015 *Nano Lett.* **15** 4628
[38] Li Z P and Xu H X 2016 *Adv. Phys. X* **1** 492
[39] Klimov V I, Mikhailovsky A A, Xu S, Malko A, Hollingsworth J A, Leatherdale C A, Eisler H J and Bawen M G 2000 *Science* **290** 314
[40] Kimov V I, Mikhailovsky A A, Mcbranch D W, Leatherdale C A and Bawendi M G 2000 *Science* **287** 1011
[41] Liao C, Xu R L, Xu Y, Zhang C, Xiao M, Zhang L, Lu C, Cui Y P and Zhang J Y 2016 *J. Phys. Chem. Lett.* **7** 4968
[42] Klimov V I, Ivanov S A, Nanda J, Achermann M, Bezel I, Mcguire J A and Piryatinski A 2007 *Nature* **447** 441